Three Dimensional Microfabricated Broadband Patch and Multifunction Reconfigurable Antennae for 60 GHz Applications

H. V. Hunerli[2,4], H. Mopidevi[1], E. Cagatay[6], M. Imbert[5], J. Romeu[5], L. Jofre[5], B. A. Cetiner[1], N. Biyikli[2,3]
[1] Department of Electrical and Computer Engineering, Utah State University, Logan UT 84322-4120 U.S.A.
[2] UNAM – National Nanotechnology Research Center, Bilkent University, Bilkent, Ankara 06800 Turkey
[3] Institute of Materials Science and Nanotechnology, Bilkent University, Bilkent, Ankara 06800 Turkey
[4] Micro and Nanotechnology Program, Middle East Technical University, Ankara 06800 Turkey
[5]Universitat Politècnica de Catalunya, 08034 Barcelona, Spain
[6]Institute for Nanoelectronics, Technische Universitat Munchen, 80333 Munich, Germany

***Abstract*— In this paper we present two antenna designs capable of covering the IEEE 802.11ad (WiGig) frequency band (57–66 GHz and 59-66 GHz respectively). The work below reports the design, microfabrication and characterization of a broadband patch antenna along with the design and microfabrication of multifunction reconfigurable antenna (MRA) in its static form excluding active switching. The first design is a patch antenna where the energy is coupled with a conductor-backed (CB) coplanar waveguide (CPW)-fed loop slot, resulting in a broad bandwidth. The feed circuitry along with the loop is formed on a quartz substrate (at 60 GHz), on top of which an SU-8-based three-dimensional (3D) structure with air cavities is microfabricated. The patch metallization is deposited on top of this structure. The second design is a CB CPW-fed loop slot coupled patch antenna with a parasitic layer on top. The feed circuitry along with the loop is formed on a quartz substrate. On top, the patch metallization is patterned on another quartz substrate. The parasitic pixels are deposited on top of these two quartz layers on top of an SU-8 based 3D structure with air cavities.**

Index Terms—beam steering, pattern reconfigurability, antenna radiation pattern, antenna measurements, multi-functional reconfigurable antennas, parasitic based antennas, 60 GHz communications.

I. INTRODUCTION

There is an increasing demand for higher data rates with upcoming WiGig wireless technology, enabling wireless data, voice and video applications at multigigabit speeds has recently been attracting much interest [1]. mm-wave frequencies, the antenna design and manufacturing poses some challenges due mainly to the small dimensions, which may be as small as 20 μm, and lossy material characteristics, which are deleterious for antenna performances. To get ahead of such effects, an efficient microfabrication approach along with appropriate material use must be adopted as well as being low-cost and compact must be taken into account.

Antennas operating at mm-wave frequencies have thus far mainly been implemented using either low temperature co-fired ceramic (LTCC) [2]–[4] or polymer substrates [5]. Although LTCC can create mechanically robust and hermetically sealed packages with high yield, it might create unwanted surface waves due to the high dielectric constant of substrate. Recently, planar antennas have also been realized on benzocyclobutene (BCB) polymers at mm waves [5]. In order to create thick enough structures, SU-8 is an excellent choice since BCB requires multiple spins to achieve desired thickness and has a very short shelf time under room temperature [6]. However, its high loss tangent is the drawback for using it as a dielectric for planar antennas. Techniques such as creating holes, air cavities, etc., to reduce the effect of dielectric loss on the antenna performance exist in the literature [7], [8]. Combining the advantages of SU-8 along with these techniques yields an antenna substrate that is both electrically and mechanically an efficient solution. Hence, in this letter, microfabricated SU-8-based three-dimensional (3D) structures with air cavities are used as low-loss alternative substrates for WiGig antennas.

II. ANTENNA DESIGN

A. Patch Antenna

The antenna as depicted in Fig. 1(a) and (b) is a CPW-fed broadband patch antenna microfabricated on an RF-compatible quartz substrate (ε_r = 3.9 tanδ = 0.0002 at 60 GHz). The feed metallization, which consists of a 50Ω- CB CPW, along with the loop is formed on a 525- μm-thick quartz substrate. The SU-8-based 3D substrate is microfabricated on top of the feed metallization as described in Section III. The 3D substrate consists of an SU-8 membrane that is supported via SU-8 posts.

The patch antenna metallization is finally formed on this 3D substrate. The location of SU-8 posts and the thickness of SU-8 membrane dictate the mechanical stability of the 3-D antenna. As SU-8 is quite lossy, an intelligent design tradeoff between the mechanical integrity of the 3D structure and the performance of the antenna needs to be incorporated. Accordingly, air cavities are incorporated in the 3D SU-8 substrate to reduce the dielectric loss, which would in turn enhance the performance of the antenna. The height of the air

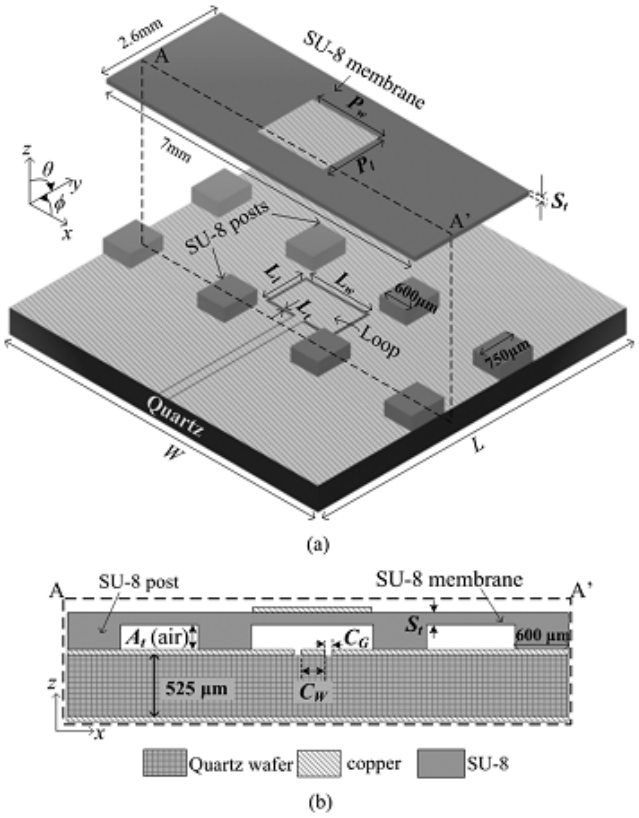

Fig.1. Schematic depicting (a) 3-D (for the sake of illustration, the SU-8 membrane is suspended on top of the CPW metallization) and (b) cross-sectional drawings of the antenna.

TABLE I. CRITICAL DESIGN PARAMETERS OF THE 3D WIGIG ANTENNA (ALL DIMENSIONS ARE IN MILLIMETERS)

W	7	P_w	1.5	L_l	0.92	C_G	0.02
L	7	P_l	1.25	L_w	1.47	C_W	0.191
L_t	0.06	S_t	0.1	A_t	0.2		

cavity, which is also the height of SU-8 posts, has an effect on the impedance BW and realized gain of the antenna.

To enhance the BW of the patch antenna, a CB CPW-fed rectangular loop slot (with dimensions L_l, L_w and L_t) couples the energy to the patch antenna. The substrate thickness of the CB CPW-fed loop slot plays an important role in broadening the radiation BW of the antenna. One of the main contributions of this letter is not only to improve the antenna performances in the WiGig band, but also to make the antenna design compatible with micro-fabrication processes, resulting in efficient and economic fabrication. Therefore, a 525- μm-thick quartz substrate, which is microfabrication-friendly as well as electrically thick to aid in broadband WiGig communication, is chosen.

The parameters of CB CPW-fed loop and patch along with those of 3D SU-8 substrate are jointly optimized to combine the patch and loop resonances, resulting in a broader BW. Also, the standard thickness of the microfabrication-

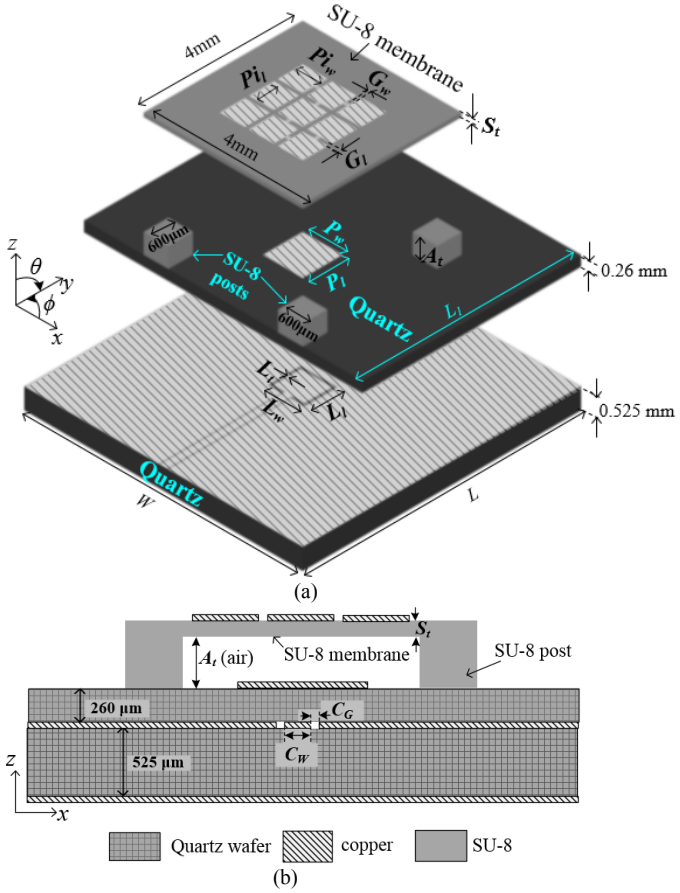

Fig.2. (a) 3D Schematic (for the sake of illustration the layers are suspended on top of each other) and (b) cross section view of the pattern reconfigurable antenna.

TABLE II. CRITICAL DESIGN PARAMETERS OF THE 3D WIGIG MRA (ALL DIMENSIONS ARE IN MILLIMETERS)

Pi_l	0.63	Pi_w	0.63	G_l	0.1	G_w	0.1
W	7	P_w	1	L_l	0.82	C_G	0.02
L	7	P_l	1	L_w	0.92	C_W	0.191
L_t	0.06	S_t	0.1	A_t	0.4	L_l	5.5

compatible quartz wafer (525 μm) is incorporated into the design optimization to attenuate possible surface waves. The methodology, taking the advantage of monolithically microfabricated 3D structures, provides greater design flexibility and cost reduction when compared to etching away portions of bulky substrates or creating vias/holes in substrates with standard thickness [9], [10].

The optimized design parameters of the patch element, CPW-fed loop, and the 3D substrate obtained from full-wave simulation. This design methodology not only minimizes the dielectric loss of SU-8 through air cavities, but also results in compact antenna size due to higher effective dielectric constant. The patch metallization on top of the SU-8 substrate focuses the electromagnetic (EM) energy to result in a

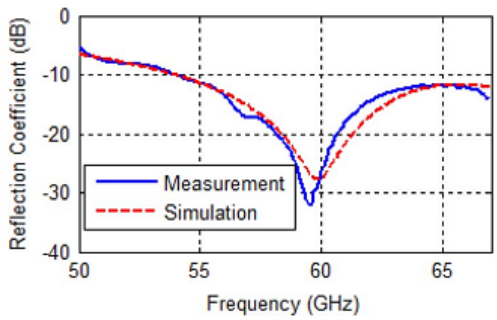

Fig.3. Simulated and measured magnitudes of S11 parameter (reflection coefficient) for a frequency range from 50 to 67 GHz obtained for the microfabricated broadband patch antenna.

narrower beamwidth, which is otherwise broader standard CPW-fed loop.

The optimized design parameters of the patch element, CPW-fed loop, and the 3D substrate obtained from full-wave simulation are provided in Table I.

B. Multifunctional Reconfigurable Antenna

In Fig. 2(a) and (b), the MRA shown is a CB CPW-fed loop slot coupled patch antenna with a parasitic layer on top with the same material properties as the patch antenna explained above. The MRA provides 9 different beam directions pertaining to: $\theta \in \{-30^o, 0^o, 30^o\}$; $\varphi \in \{-45^o, 0^o, 45^o, 90^o\}$ over 59 – 66 GHz band. The antenna structure consists of a broadband patch antenna sourced by a CB CPW fed loop slot. The CB CPW fed loop slot and patch metallization are formed on two quartz substrates (ε_r = 3.9, tan δ = 0.0002 at 60 GHz) with thicknesses of 525µm and 260µm, respectively. An SU-8 based three-dimensional (3D) structure with air cavities is micro-fabricated on top of the 260µm quartz substrate with the goal of forming a reconfigurable parasitic layer on top. This reconfigurable parasitic layer consists of 3x3 metallic rectangular shaped metallic pixels which are connected or disconnected through perfect open/short metallic strips.

The critical design parameters of the 60 GHz MRA obtained from full-wave simulation are given in Table II.

III. MICROFABRICATION

A four and a five mask level, microwave-compatible microfabrication process is developed utilizing 3D thick SU-8 coating and patterning processes as well as standard thin-film deposition and patterning/etching processes for the patch antenna and the MRA respectively. Prior to fabrication, 4-inch RF-compatible/low-loss quartz substrates were cleaned using standard acid/solvent cleaning, DI-water rinsing, nitrogen-blow drying, and dehydration baking on a 120 C hotplate.

The fabrication process of the patch antenna can be summarized as following: 1) physical vapor deposition (PVD)

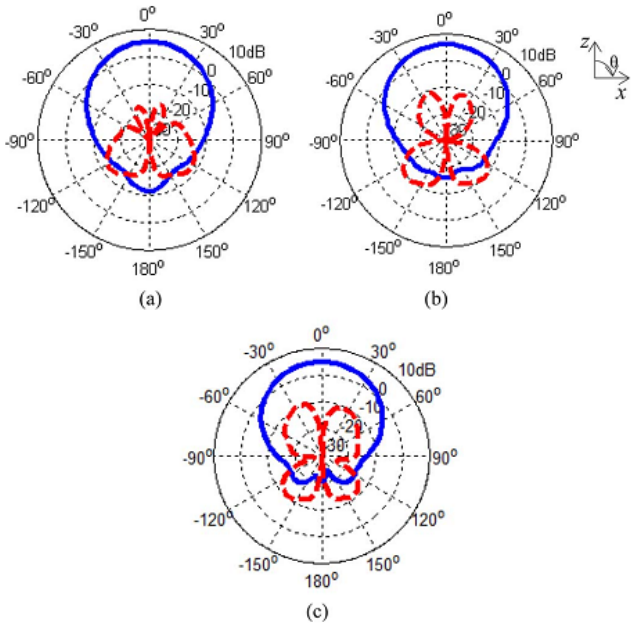

Fig.4. Simulated realized gain plot (dB) of the antenna in -plane at (a) 57, (b) 62, and (c) 66 GHz.

and patterning of the CPW metal layer that was formed of titanium/copper (Ti/Cu) where Ti functioned as the 10-nm-thick adhesion layer and Cu thickness was 300 nm. After the metallic CPW was formed using sputtering, 2) blank Ti/Cu deposition on the backside of quartz wafer was implemented, which functioned as the ground metal layer. 3) Later, SU-8 coating and patterning process consisting of two mask layers was carried out. A 300- µm-thick SU-8 layer was reached using two consecutive spin coatings of 150-µm layers and soft-baked at 95 C after each layer deposition, which was followed by two separate exposures. The first (second in the overall process) mask was used to cross-link the post regions. A lower exposure dose was used in the second (third mask in the overall process) mask with the aim of cross-linking only the 100-µm upper layer of the membrane areas. Immediately after the exposure steps, a post-exposure bake (PEB) was applied with sufficient ramp-up and ramp-down durations to minimize the stress accumulation within the structural SU-8 layers. 4) Patch metal deposition and patterning followed using -nm-thick Cu DC-sputtering and wet-etch patterning using the fourth lithography mask. Finally: 5) the sample is soaked into SU-8 developer solution within an ultrasonic bath, targeting to dissolve and remove the uncross-linked SU-8 layer underneath the partially exposed membrane.

The fabrication process of the MRA consisting of 5 mask levels can be summarized as following: 1) Sputtering and patterning of the CPW metal layer that was formed of chromium/copper (Cr/Cu) where Cr functioned as the 10-nm-thick adhesion layer on the 525 µm quartz substrate and Cu thickness was 300 nm. After the metallic CPW was formed using sputtering, 2) blank Cr/Cu deposition on the backside of quartz wafer was implemented, which functioned as the ground metal layer. 3) Sputtering and patterning of the patch

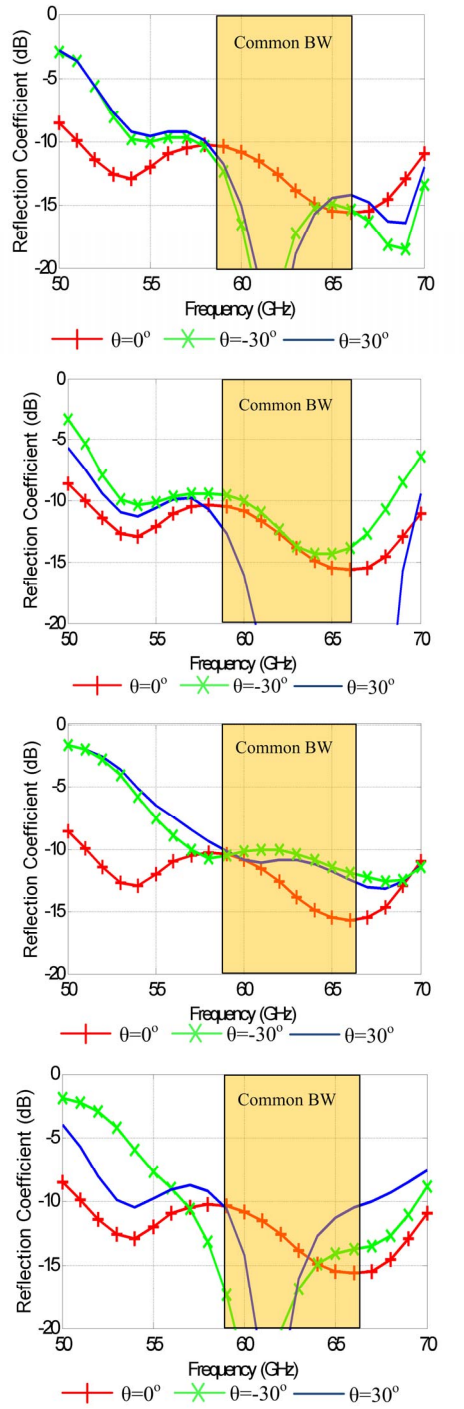

Fig.5. The simulated reflection coefficient of the MRA in (a) φ = 0 (xz) plane (b) φ = 45 plane (c) φ = 90 (yz) plane (d) φ = -45 plane

metallization was formed using Cr/Cu on the 260 µm quartz substrate. 4) Later, SU-8 coating and patterning process consisting of two mask layers was carried out. A 500- µm-thick SU-8 layer was reached using two consecutive spin coatings of 250-µm layers and soft-baked at 95 C after each layer deposition, which was followed by two separate

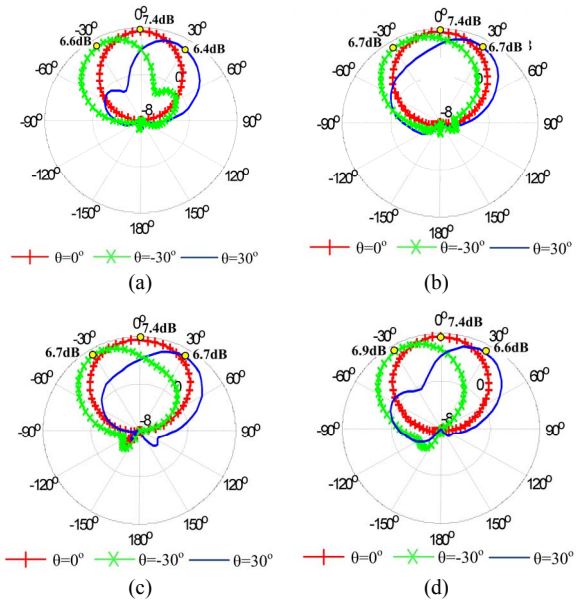

Fig.6. The simulated total gain plot (in dB) of the MRA at 60 GHz in (a) φ = 0 (xz) plane (b) φ = 45 plane (c) φ = 90 (yz) plane (d) φ = -45 plane

exposures. The first (third in the overall process) mask was used to cross-link the post regions. A lower exposure dose was used in the second (fourth mask in the overall process) mask with the aim of cross-linking only the 100- µm upper layer of the membrane areas. Immediately after the exposure steps, a 5-min PEB was applied with sufficient ramp-up and ramp-down durations to minimize the stress accumulation within the structural SU-8 layers. 4) Parasitic pixel metal deposition and patterning followed using 300-nm-thick Cu DC-sputtering and wet-etch patterning using the fifth lithography mask. 6) The sample is soaked into SU-8 developer solution within an ultrasonic bath, targeting to dissolve and remove the uncross-linked SU-8 layer underneath the partially exposed membrane. Finally, the 525 µm thick patterned sample is bonded to the 260 µm thick quartz with 3D SU-8 structure on it.

IV. Measurements and Characterizations

The performance of the microfabricated loop-coupled patch antenna with CPW feed has been measured with an Agilent 8510C vector network analyzer (VNA) together with a GSG-probe station from 50 to 67 GHz. The pitch of the probes (distance between one ground tip and the signal tip) is of 150 µm. The CPW feeding lines of the patch antenna were designed to perfectly accommodate to this probe pitch. One port calibration process was performed manually, measuring three known standards (i.e., open, short, and broadband matched load terminations) in order to establish the measurement reference planes. The wafer with the microfabricated patch antenna prototypes was placed over the sample stage. Since the antenna was designed with a CB CPW feed, the effect of the metal plate of sample stage in the measurement setup has been minimized. The sample stage has

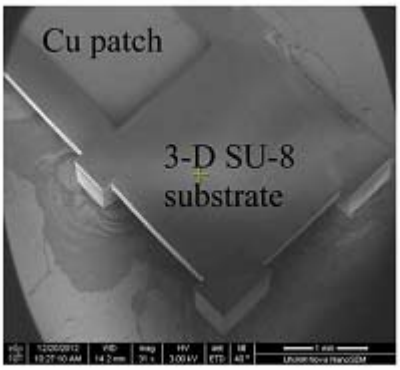

Fig.7. Angled-view SEM micro-graph of a completed patch antenna

Fig.8. Angled-view SEM micro-graph of a completed MRA

a movable metal plate that allows probes to contact anywhere on the wafer surface with precise motion in a 2-D plane (xy-directions). The stage is equipped with a vacuum chuck to fix the wafer to the metal plate, with the aim to ensure the perfect contact of the probe tips with the CPW feeding the patch antenna. A PC communicates with the VNA in order to control the process, run the calibration software, and stores the measurements. The simulated and measured reflection coefficients for the patch antenna, with good agreement between them, are plotted in Fig. 3 for a frequency range from 50 to 67 GHz. Slight variations between measured and simulated results can mainly be attributed to the fabrication tolerances. The reflection coefficient shows that the antenna has a 2:1 VSWR BW of greater than 9 GHz (~15% of fractional BW), which covers the entire frequency range of the IEEE 802.11ad (57–66 GHz). The simulated radiation patterns of the linearly polarized antenna in xy-plane at 57, 62, and 66 GHz are shown in Fig. 4(a)–(c), respectively, showing a patch-type pattern, as expected. The cross-polarization level is at least 16 dB below the co-polarization level of the antenna. The realized maximum gain of the antenna is relatively constant and is in the range 5.5–7 dB over the entire BW. Higher gain is obtained due to the presence of air cavities in the 3D SU-8 substrate, which effectively reduces the dielectric loss. The simulated reflection coefficients for the MRA are plotted in Fig. 5 (a)-(d) for a frequency range from 50 to 70 GHz. The reflection coefficient shows that the MRA has a BW of 7 GHz (~11.7% of the fractional BW) in (a) $\varphi = 0$ (xz) plane, (b) $\varphi = 45$ plane, (c) $\varphi = 90$ (yz) plane and (d) $\varphi = -45$ plane. The total gain plot simulations of the MRA at 60 GHz are given in Fig. 6 (a)-(d) in (a) $\varphi = 0$ (xz) plane (b) $\varphi = 45$ plane (c) $\varphi = 90$ (yz) plane (d) $\varphi = -45$ plane.

Fig.7 and Fig.8 shows scanning electron microscope photographs of the completed patch antenna and MRA.

V. CONCLUSIONS

A CPW-fed broadband patch antenna and MRA compatible with IEEE 802.11ad standard (WiGig) is designed and microfabricated. The measured reflection coefficient data of the patch antenna is in good agreement with the simulation giving ~15% BW. The simulated radiation patterns with reasonably constant gain values (5.5–7 dB) in the broadside direction over the entire WiGig band (57–66 GHz) indicate a design with low dielectric loss. The microfabricated MRA is subject to characterization in the following weeks. The SU-8-based 3-D microfabrication processes developed for this antenna structure provides an important advantage for custom-made reconfigurable antennas that might also be greatly useful in WiGig applications.

REFERENCES

[1] C. J. Hansen, “WiGig: Multi-gigabit wireless communications in the 60 GHz band,”IEEE Wireless Commun., vol. 18, no. 6, pp. 6–7, Dec. 2011.

[2] T. Seki, N. Honma, K. Nishikawa, and K. Tsunekawa, “A 60-GHz multilayer parasitic microstrip array antenna on LTCC substrate for system-on-package,” IEEE Microw. Wireless Compon. Lett. , vol. 15, no. 5, pp. 339–341, May 2005.

[3] Y.P.Zhang,M.Sun,K.M.Chua,L.L.Wai,D.Liu,andB.P.Gaucher, “Antenna-in-package in LTCC for 60-GHz radio,” in Proc. IEEE Int. Workshop Antenna Technol., Mar. 2007, pp. 279–282.

[4] S. Wi et al., “Package level integrated antennas based on LTCC technology,” IEEE Trans. Antennas Propag., vol. 54, no. 8, pp. 2190–2197, Aug. 2006.

[5] S. Seok;, N. Rolland, and P.-A. Rolland, “Millimeter-wave quarter-wave patch antenna on benzocyclobutene polymer,” in Proc. 38th Eur. Microw. Conf. , Oct. 27–31, 2008, pp. 1018–1021.

[6] A.-D. Campo and C. Greiner, “SU-8: a photoresist for high-aspect-ratio and 3D submicron lithography,” J. Micromech. Microeng., vol. 17, pp. R81–R95, 2007.

[7] G. P. Gauthier, A. Courtay, and G. M. Rebeiz, “Microstrip antennas on synthesized low dielectric-constant substrates,”IEEE Trans. Antennas Propag., vol. 45, no. 8, pp. 1310–1314, Aug. 1997.

[8] D. R. Jackson, J. T. Williams, and A. K. Bhattacharyya, “Microstrip patch designs that do not excite surface waves,”IEEE Trans. Antennas Propag., vol. 41, no. 8, pp. 1026–1037, Aug. 1993.

[9] G. P. Gauthier, A. Courtay, and G. M. Rebeiz, “Microstrip antennas on synthesized low dielectric-constant substrates,”IEEE Trans. Antennas Propag., vol. 45, no. 8, pp. 1310–1314, Aug. 1997.

[10] D. R. Jackson, J. T. Williams, and A. K. Bhattacharyya, “Microstrip patch designs that do not excite surface waves,”IEEE Trans. Antennas Propag., vol. 41, no. 8, pp. 1026–1037, Aug. 1993.